Optimizing the Locations of Electric Taxi Charging Stations: a Spatial-temporal Demand Coverage Approach

Abstract: Vehicle electrification is a promising approach towards attaining green transportation. However, the absence of charging stations limits the penetration of electric vehicles. Current approaches for optimizing the locations of charging stations suffer from challenges associated with spatial-temporal dynamic travel demands and the lengthy period required for the charging process. The present article uses the electric taxi (ET) as an example to develop a spatial-temporal demand coverage approach for optimizing the placement of ET charging stations in the space-time context. To this end, public taxi demands with spatial and temporal attributes are extracted from massive taxi GPS data. The cyclical interactions between taxi demands, ETs, and charging stations are modeled with a spatial-temporal path tool. A location model is developed to maximize the level of ET service on the road network and the level of charging service at the stations under spatial and temporal constraints such as the ET range, the charging time, and the capacity of charging stations. The reduced carbon emission generated by used ETs with located charging stations is also evaluated. An experiment conducted in Shenzhen, China demonstrates that the proposed approach not only exhibits good performance in determining ET charging station locations by considering temporal attributes, but also achieves a high quality trade-off between the levels of ET service and charging service. The proposed approach and obtained results help the decision-making of urban ET charging station siting.

Keyword: facility location; spatial-temporal demand; maximum coverage; big data; electric vehicle

1. Introduction

Currently, the transportation sector contributes 20% to 30% of the total production of greenhouse gases (GHGs) such as oxocarbons (CO_2 and CO) and nitrous oxide (N_2O) (IPCC, 2013). The reduction of GHGs in the transportation sector has therefore gained much attention from with respect to technical innovation and scientific research. Among various alternatives, vehicle electrification is a promising approach towards attaining green transportation (IEA, 2014a). However, relative to alternative fuel vehicles, electric vehicles (EVs) generally have a shorter range that is compounded by the requirements of an extended charging period (IEA, 2013), which, with the absence of charging infrastructure, inspires a severe degree of anxiety regarding the allowable vehicle range (i.e., range anxiety). Meanwhile, the return of the considerable investment required for charging stations is exceedingly meager under conditions of low EV penetration (Carpenter et al., 2014). Therefore, the EV market is dropping into a kind of “egg-chicken” paradox (Hiwatari et al., 2011; Xi et al., 2013; Jung et al., 2014). Clearly, the relationship between active EVs and available EV charging stations must be carefully coordinated (Nie and Ghamami, 2013; Sathaye, 2014).

Public transportation, such as bus and taxi, are an appropriate first step towards electrification (IEA, 2013), and various cities have made efforts in this direction (IEA, 2013). For example, London plans to substitute all taxis in the city with EVs with the aim of low carbon emissions (IEA, 2014b). New York issues roadmap for electrifying one-third of the city’s taxi fleet by 2020 (NYC TLC, 2013). In China, the city of Shenzhen plans to add 3000 electric taxis (ETs) by 2015 (Shenzhen Transportation Administration, 2012). Therefore, the emerging question is where to locate charging stations to serve the various charging demands of a city.

Location approaches are used to address the facility location problem to serve geographically distributed demands (Church, 2002). These methods typically consist of two main components: a demand representation and a location model. Usually, the demand is represented as points, polygons, or flow in a spatial context (Miller, 1996). The magnitude of the demand is generated by a synthetic method based on population or travel surveys. Demand is defined as being covered (i.e., fullfilled) if it is within a certain travel distance/time to a facility (Church and ReVelle, 1974). A location model is designed to select the best locations that achieve maximum system utility, minimum cost, or other objective(s). Based on various demand representations and objectives, a number of location models have been proposed such as the *p-Median* (Hakimi, 1964), *p-Center* (Hakimi, 1964), the *maximum coverage location problem* (MCLP; Church and ReVelle, 1974), and the *flow capture location model* (FCLM; Hodgson, 1990). With the aid of geographic information systems (GISs) in the integration of spatial data management, visualization, and analysis, location models and optimization methods have been implemented and widely applied for facility location in public and private sectors (Thill, 2000; Church, 2002; Drezner and Hamacher, 2004; Church and Murray, 2009; Gentili, M., Mirchandani, P.B., 2012).

For appropriately locating ET charging stations, however, time is a crucial factor. Firstly, daily taxi demand exhibits spatial-temporal variations from hour to hour and from place to place (Wong et al., 2014; Qian and Ukkusuri, 2015). This type of spatial-temporal dynamic feature is quite difficult to capture using a synthetic demand approach, and has therefore been ignored in current demand representation methods (Miller, 1996; Church, 2002). This feature also creates a substantial challenge for defining the conditions whereby a charging demand is fulfilled, or formally, is covered (Zhou and Lin, 2012). The acquisition of spatial-temporal variations in taxi demand is a basic issue. Secondly, the required duration for ET charging at charging stations can be quite long, where, depending on the charging mode, the charging duration can be from 5 minutes to several hours (IEA, 2013). Such an extensive duration will heavily affect the interaction between taxi demand and available ETs. Moreover, the capacity of a charging station is limited, depending upon the number of charging stakes, and only a limited number of ETs can be charged simultaneously at a given charging station. Any ETs in excess of the maximum service number arriving at a station for charging must therefore wait for service (Qin and Zhang, 2013), which would also affect subsequent ET service on the roads. However, traditional location models cannot address these temporal issues at a facility. Clearly, an extension of the conventional location model is needed.

Detailed-rich space-time data is an aid to decision-making and policy analysis. Recently, taxis with GPS that track real-time vehicle positions have been widely applied in transportation (Tu et al., 2010; Li et al., 2011; Fang et al., 2011; Zhang et al., 2013; Yue et al., 2014). Data regarding taxi service with corresponding time information in a city could be extracted from raw taxi GPS data. This information would not only contribute to traffic monitoring (Li et al., 2011), travel time estimation (Zhan et al., 2013; Rahmani et al., 2015), etc., but also deepen our understanding of travel patterns (Liu et al., 2010), urban taxi service (Qian and Ukkusuri, 2015), use of critical infrastructure (Fang et al., 2013, 2015), etc. Such time rich information also provides an opportunity to capture city-wide spatial-temporal variations in taxi demands, which could serve as the cornerstone for the optimal siting of ET charging stations.

The present article develops a spatial-temporal demand coverage approach using big spatial-temporal data to facilitate charging station siting. To this end, actual spatial-temporal taxi demands in the city of Shenzhen, China has been extracted from large volume raw taxi GPS data. Using the spatial-temporal path concept, the cyclical taxi demand serving on the roads, ET charging, and possible additional ET waiting at charging stations are modeled in a spatial-temporal context. A spatial-temporal demand coverage location model is proposed according to considerations of EV range, the requirements of charging and waiting at charging stations, and the competition of taxies. Only the taxi demand covered by an ET is included in the presented model. Analysis of the obtained results for Shenzhen, China indicates the good performance of the proposed ET charging station siting approach obtained by taking the time dimension into account. The daily reduced carbon emission (RCE) generated by the ETs with located charging stations is also mapped to evaluate the green effect.

The remainder of this article is organized as follows. The next section reviews existing location approaches and their applications to charging station siting. Section 3 describes the study area and associated data. Section 4 presents the proposed spatial-temporal demand coverage approach. Section 5 illustrates the obtained results, and analyzes the environmental effect of used ETs with located charging stations. In the final section, we discuss and conclude the study.

2. Literature review

Facility location begins with a representation of human demands and locates facilities at the places best suited to serve those demands. According to the demand representation, current location approaches are divided into two approaches: point demand and flow demand. This section briefly reviews the two approaches and their implementations in charging station siting. For comprehensive reviews related to facility location, please refer to Church (2002), ReVelle & Eiselt (2005), and Murray (2010).

2.1 Point demand location approach

The *point demand location approach* assumes that demand is located at distinct places, such as residential areas, working places, and shopping centers. The basic demand unit is a polygonal area based spatial object in a geographical space (Church and Murray, 2009). The demand count or the demand density is usually derived from demographic data, topographic data, cadastral data, survey data, etc. Because a polygonal area is much too complex for geocomputing, the representation of the demand is usually simplified as a point at the center of the polygon by abstracting and aggregating (Tong and Murray, 2009). The inherent assumption is that dedicated travels between demand locations and facilities are made to fulfill geographical distributed needs. Therefore, the travel distance/time is defined as the key system utility index. The demand unit is defined as covered if it is within a certain travel distance/time to facilities. The objective is to either minimize the total travel cost between demands and facilities (the *p-Median*; Hakimi, 1964), minimize the maximum travel cost (the *p-Center*; Hakimi 1964; Biazaran and SeyediNezhad, 2009), maximize the demand coverage with a given number of facilities (MCLP; Church and ReVelle, 1974; Drezner and Hamacher, 2004), or optimize some other objectives relating to point demands. Thus far, the point demand location approach has been widely employed in various decision making applications such as the siting of warning sirens (Tong and Murray, 2009; Wei and Murray, 2014), bicycle stations

(García-Palomares et al., 2012), roads (LI et al., 2009).

Although the point demand location approach has achieved success in many applications, it still faces a number of challenges in transportation such as fuel station siting and charging station locating, e.g., the demand occurring during a trip rather than a fixed place, the cost index, etc. Rather than engaging in dedicated travels between individual facilities and customer locations to procure services, drivers may prefer to fulfill side needs during a long trip (Wang and Wang, 2010). Also, travel distance/time as the cost in the point demand location approach is not an appropriate measure for the system cost in location modeling in transportation. Therefore, both the point demand representation and the covering definition are inaccurate in this scenario. A new location model is therefore needed to effectively handle this type of location problem.

2.2 Flow demand location approach

The *flow demand location approach* assumes that consumers search for a service during the travel to their destination locations (Hodgson, 1990; Kuby, 2006). In this approach, the basic demand unit is not a polygon-based or a point-based spatial object representing aggregated human needs, but, rather, demand is represented as a flow passing along consumer routes of travel (Upchurch and Kuby, 2010). Formally, this location approach is denoted as the FCLM (Hodgson, 1990), which seeks to locate some facilities to intercept as many demand flow pathways as possible. In this method, an origin-destination matrix is typically first generated to model the demand distribution in the study area. The demand is defined as covered when a facility is located at any point along a consumer travel pathway. Because the objective is to locate facilities to maximize the passing demand flow, the FCLM is well suited for the types of facilities where consumers are served on their routes to travel destinations (Upchurch and Kuby, 2010; Zeng et al., 2010).

With considerations for limited travel distance, the FCLM has been extended to the flow-refueling location model (FRLM; Kuby et al., 2009) that locates a given number of stations to maximize the number of trips that can be refueled during a long travel. Because refueling is also considered, this model is more effective for a larger study area (Capar et al., 2013). Both FCLM and FRLM have been successfully applied to the transportation sector in the optimal siting of conventional and alternative fuel stations (Goodchild and Noronha, 1987; Kuby, 2006; Kuby et al., 2009; Lim and Kuby, 2010; Kim and Kuby, 2013). However, these methods consider only the spatial dimension of demand, and the temporal dimension of demand is ignored, such as the time of demand, service duration, and the possible waiting at a facility.

2.3 charging stations siting

Recently, both location approaches have been used for charging station siting. Frade et al. (2011) used the MCLP model for optimal siting of public charging stations using household travel survey data for Lisbon, Portugal. Cruz-Zambrano et al. (2013) implemented the FCLM to locate fast charging stations in Barcelona, Spain. Xi et al. (2013) determined charging demand from demographic data, and employed a simulation-optimization approach to optimize the number of charging stakes at candidate places for public EV charging. However, the determination of travel demand in these applications of location modeling is still conducted without time information. You and Hsieh (2014) developed a location model based on round-trip itineraries for public EV charging station siting to serve a maximum number of trips. Nevertheless, potential waiting at the facility was not modeled.

To date, Jung et al. (2014) have conducted the only study where the potential waiting time of ETs, based on random itinerary information over an 8 hour period in Seoul, Korea, was considered to optimize the configuration of charging stations for ETs. However, the stochastic demand data were synthesized using transportation planning software, which deviates substantially from reality. Detailed spatial-temporal taxi demand data is expected to obtain better results. The present study extracted actual taxi travel demand from massive taxi GPS data to model the space-time interaction between taxi demands, ETs, and charging stations. A spatial-temporal demand coverage location model is developed to site ET charging stations in a space-time GIS environment, which benefits decision-making regarding ET charging station.

3. Study area and data

The research was conducted in Shenzhen, a metropolitan area in South China, as shown in Fig. 1. To reduce carbon emission in the transportation sector, the local administration of Shenzhen plans to implement the use of ETs. Numerous ET charging stations are expected to be built. In this study, we propose a spatial-temporal demand coverage location approach using massive taxi GPS data to facilitate the siting decision-making. Raw taxi GPS data, the transportation network, the ET, and charging station data are used. The details of the data are described as follows.

-*Taxi GPS data*. Every day in Shenzhen, about 15,000 taxis are actively engaged in transferring people between various locations such as homes, workplaces, shopping centers, the airport, and parks. According to transportation statistics, about 420,000 to 460,000 trips are conducted daily by taxis, which is about 5% of the travel occurring in Shenzhen. Each taxi has been installed with a smart terminal connected with a GPS receiver, which records data concerning the vehicle identification, time, position, speed, and working status with a sampling interval between 40 to 80 seconds. Table 1 describes the taxi GPS format, and provides an example. In particular, the working status is a binary variable indicating whether or not the taxi is serving a client at a given time, where the status is recorded as 1 if the taxi is occupied, and 0 otherwise when the taxi is vacant. Therefore, both the times and locations at which passengers are picked-up and dropped-off can be identified from the taxi GPS data. In the present study, we employed raw taxi GPS data for a seven-day period from Oct. 12, 2013 to Oct. 18, 2013 to extract historical spatial-temporal dynamic taxi demands.

[place Tab. 1 about here]

[place Fig. 1 about here]

-*The transportation network*. The transportation network, derived from a professional navigation company, NavInfo, China, and displayed in Fig. 1, was modeled as a directed graph including 13,107 nodes and 20,783 edges. The data was used to recover taxi trajectories and extract dynamic taxi demands.

-*The electric taxi*. The ET employed in Shenzhen is the E6 model produced by BYD (Build Your Dream) Auto Co., Ltd. With a battery charged at full capacity, BYD E6 can travel up to 250 km. The charging time of the E6 varies from 1 h to 3 h depending upon the charging mode.

-*The charging stations*. A charging station has multiple charging stakes, which transfer power from the grid to an ET. The number of stakes indicates a station's charging capacity. Formally, a charging station s is defined as $<x,y,n>$, where (x, y) is the location and n is the number of stakes. The space occupied by the charging station is omitted by simplifying it as a point. We set n to 50 according to the guide from Shenzhen transportation administration.

4. The spatial-temporal demand coverage approach for ET charging station siting

The presented location approach for ET charging station siting extends the demand representation and the location model into a spatial-temporal context. It makes use of massive taxi GPS data for optimizing the placement of ET charging station. Fig. 2 illustrates the workflow of the approach. Firstly, dynamic taxi demands are extracted from the raw GPS data in conjunction with the transportation network data. The cyclical interaction between taxi demands, ETs, and charging stations in the spatial-temporal context is modeled with a spatial-temporal path tool which depicts an individual's sequential activities at various locations over a time period (Hägerstrand, 1970). Then, a spatial-temporal demand coverage location model (STDCLM) is proposed to maximize ET service on the roads and charging service at the stations. A genetic algorithm is used to solve the STDCLM. Finally, the obtained results are analyzed, including the spatial pattern of covered demands, the temporal pattern of demand serving, charging and waiting behaviors, the impact of charging speed, the marginal utility, and the daily RCE estimation.

Basic assumptions about ETs and charging stations are: (1) all ETs have the identical electricity capacity, E; (2) with full capacity electricity, all ETs have the same maximum travel distance, D_{max}; (3) the charging speed CS for all ETs in any located station are identical. It indicates that time E/CS will be cost to recharge an ET from the zero-electricity state to the full capacity electricity. It also specifies that all charging stations provide the same charging service; (4) once a charging process begins, it can't be interrupted or stopped until the charging need is completely fulfilled; (5) the travelable distance d is proportional to the remaining capacity e (Dong et al., 2014), as given in equation (1), where $0 \le e \le E$. In other words, the remaining electricity is linearly reduced with the traveled distance.

$$d = D_{\max} e / E \tag{1}$$

[place Fig. 2 about here]

4.1 Taxi demand and taxi travel

In contrast to point demand or flow demand, taxi demand is based on a client's plan to travel from some origin to a given destination at some time. Formally, the taxi demand can be defined as the triplet $TD = \langle t_o, (x_o, y_o), (x_d, y_d) \rangle$, where t_o denotes the beginning time of the demand, (x_o, y_o) denotes the spatial location of the origin, and (x_d, y_d) denotes the spatial location of the destination.

To accommodate a travel demand, a taxi picks up a client at the origin, makes a dedicated transit to the destination, and drops off the client. Formally, taxi travel can be represented by extending the taxi demand to the quintuplet $TD = \langle t_o, (x_o, y_o), path, t_d, (x_d, y_d) \rangle$, where the *path* denotes the driving route from the origin to the destination, and t_d is the arrival time at the destination.

All taxi demands and taxi travels in the city are extracted from the massive raw taxi GPS data. To this end, spatial-temporal trajectories are firstly recovered using the map-matching algorithm of Li et al. (2011). Then, in accordance with changes in a taxi's working status, the origin and the destination of a taxi demand is identified. Based on the time-series GPS records for a taxi listed in Table.1, if the working status shifts from 0 to 1, a taxi demand *TD* is generated in the spatial-temporal context. The recorded position is (x_o, y_o) of *TD*, and the recorded time is t_o. After encountering a series of GPS records with a status of 1, the taxi arrives at the destination of *TD* whereupon the status shifts to 0. The last record with a status 1 labels (x_d, y_d) and t_d. The sequence of road links traversed from the origin to the destination is the *path*, which preserves the effect of numerous factors, such as road conditions, traffic congestion, and drivers' personal preferences. After processing of all raw GPS data, all taxi demands and taxi travel data with exact spatial-temporal information are stored in a database for charging station siting.

4.2 The interaction between taxi demands, electric taxies and charging stations

When substituting a number of ETs into the current oil-based fuel taxi system, both ET drivers and oil-based fuel taxi drivers explore dynamically changing demands to provide good taxi service to the public. If a taxi demand is serviced by an ET, we define the taxi demand as *covered* by the ET. To identify taxi demands covered by ETs, we model the daily ET lifecycle using the spatial-temporal path tool, which illustrates the spatial-temporal interaction between taxi demands, ETs and charging stations. Fig. 3 gives an example of the spatial-temporal paths of ETs. Following the sequence of ET driver's activities, an ET continues serving taxi demands (TD_1, …, TD_n in Fig.3) when the remaining electricity is enough (e.g., after serving TD_i in Fig.3). Otherwise, the ET goes to a charging station. According the charging state of charging station at the arrival time, the charging will be done immediately (l_1 in Fig.3) or after an essential waiting (l_3 in Fig.3). The details of interactions are described below.

[place Fig. 3 about here]

4.2.1 Taxi demand coverage and charging decision

With sufficient electrical power, the ET serves emerging taxi demands for the public. An idle ET at a position (x, y) at a time t rationally seeks a taxi request from the emerging demands nearby its current location. To model the competition between taxis, we identify the covered demand from a set of spatially near demands. The roulette wheel selection rule is used to determine which demand will be served by the ET to simulate the uncertainty in actual taxi service. An uncovered demand neighbor list nearby (x, y) after time t is first filled according to distance criteria. Then, a random value δ within [0, 1] is generated to select the *ith* nearest demand TD_i from the list to serve, as given by equation (2), where a_i is the accumulated probability that the *ith* nearest demand is served in historical taxi serving.

$$a_i < \delta \le a_{i+1} \tag{2}$$

Whether or not the current charge state of the ET is sufficient to serve the selected demand TD_i is examined before initiation of taxi travel. If the ET's current charge state e_{to} is greater than the threshold required for traveling to the nearest charging station after serving TD_i, the demand will be covered. The demand is covered by picking up the client at the corresponding (x_o, y_o) and t_o of TD_i, traversing the *path*, and arriving at (x_d, y_d) at t_d. Afterwards, the space-time position of the ET is updated with (t_d, x_d, y_d) of TD_i. The remaining charge capacity e_{to} is updated by equation (3), where d_{td} is the length of the corresponding driving path. Otherwise, the taxi demand is rejected and the ET travels to the nearest charging station for battery recharging. The remaining charge capacity when arriving a charging station will be updated according to the travel to the charging station.

$$e_{t_d} = e_{t_o} - d_{td} E / D_{max} \tag{3}$$

4.2.2 Charging at the station

The charging of an ET at a station is decided by the arrival time and current charge state at the station. If an idle charging stake is found at the station, the charging action will begin at once when ET v arrives at time T_v^a. The charging duration is determined by the remaining charge capacity e_v, the expected charge capacity e'_v and *CS*. In this paper, we set e'_v as a random value within [0.95*E*, *E*] to model the diversity of charging decisions. The charging duration tc_v of v is given by equation (4). The charging of v will be end at time $T_v^e = T_v^a + tc_v$. Finally, the ET's charge state e_v is updated with the value e'_v. After charging, the ET will return to serving the taxi demand in the city.

$$tc_v = (e'_v - e_v)/CS \tag{4}$$

4.2.3 Waiting at the station

In the absence of an idle charging stake at the station, ET v must wait until a charging ET in the station completes its charging action and releases a stake. In this case, the wait time t_w for v is equal to the difference between the arrival time T_v^a and the earliest charging completion time at the station $\min_{u \in V_s} T_u^a$, as given by equation (5), where u denotes a charging ET at a station s and V_s denotes the set of charging ETs at s at time T_v^a. Based upon equations (4) and (5), the charging for v will end at time $T_v^e = T_v^a + tw_v + tc_v$. After charging, the ET leaves the station and proceeds to serve taxi demands on the roads.

$$tw_v = \min_{u \in V_s}\left(T_u^e\right) - T_v^a \tag{5}$$

Owing to the cyclical demand serving, vehicle charging, and waiting, the siting of charging stations will heavily affect public ET service and the charging service for ET drivers.

4.3 The spatial-temporal demand coverage location model

The STDCLM aims to locate a set of ET charging stations to maximize both the ET service level and the charging service level. The ET service level is indicated by the ET covered taxi demands, and we measure it according to the total distances of the taxi travel of all ET covered taxi demands. The longer the total distances, the better is the level of ET service. The charging service level is indicated by the extent to which

ET drivers must wait to charge at charging stations, and we measure it according to the total wait time at all charging stations. The lower the total wait time, the better is the level of charging service. It should be mentioned that travel distance/time to located stations is not explicitly included in the STDCLM. Reasons are from two aspects. Firstly, a survey of ETs on taxi drivers in Shenzhen, China, indicates that, because of the lengthy period required for the charging process, drivers care more about the waiting time at stations than the travel time to/from stations. Secondly, as Fig. 3 illustrates, in order to calculate the total taxi travel distances of all ET covered demands, the travel distances to charging stations (D_n to the charging station in Fig.3) have been subtracted from the total travel distances.

The mathematical formulation of the STDCLM is as below.

$$Maximize \ F = \sum_{t\in T}\sum_{v\in V}\sum_{q\in Q} x_{vqt} d_q - \lambda \sum_{t\in T}\sum_{v\in V} t w_{vt} \tag{6}$$

Subject to:

$$\sum_{t\in T}\sum_{v\in V} x_{vqt} \le 1 \quad \forall q\in Q \tag{7}$$

$$\sum_{v\in V} y_{vst} \le n \quad \forall s\in S, \forall t\in T \tag{8}$$

$$\max(y_{vst}) = z_s \quad \forall s\in S \tag{9}$$

$$\sum_{s\in S} z_s = M \tag{10}$$

$$\begin{gathered} d_v^{t,t'} = (e_v^{t'} - e_v^{t}) D_{\max}/E \quad \forall v\in V, t<t' \\ e_v^{t} \ge E_{\min}, e_v^{t'} \ge E_{\min} \end{gathered} \tag{11}$$

$$x_{vqt} = \{0,1\} \quad \forall v\in V, \forall q\in Q, \forall t\in T \tag{12}$$

$$y_{vst} = \{0,1\} \quad \forall v\in V, \forall s\in S, \forall t\in T \tag{13}$$

$$w_{vt} = \{0,1\} \quad \forall v\in V, \forall t\in T \tag{14}$$

$$z_s = \{0,1\} \quad \forall s\in S \tag{15}$$

Here, S is the set of candidate locations to site charging stations, Q is the set of spatial-temporal taxi demands, V is the set of ETs, T is the time period, n is the number of stakes in a charging station, M is the number of charging stations to be located, q is a taxi demand, and d_q is the taxi travel distance (/km) from q's origin to the destination. In addition, we employ the following binary variables, where x_{vqt} is 1 if q is covered by v at a time t, and is 0 otherwise; y_{vst} is 1 if v is charging at s at time t, and is 0 otherwise; w_{vt} is 1 if v is waiting at s at time t, and is 0 otherwise; z_s is 1 if s is to be located and is 0 otherwise. Furthermore, $d_v^{t,t'}$ is the accumulated travel distance of v within a time window [t, t'], where t is the leaving time from a station after the *ith* charging, and t' is the arrival time at a station for the *(i+1)th* charging event.

The objective of (6) is to maximize the ET service level and the charging service level. The expression $\sum_{t\in T}\sum_{v\in V}\sum_{q\in Q} x_{vqt} d_q$ (km) is the total taxi travel distance of all ET covered taxi demands, indicating the ET service level, and $\sum_{t\in T}\sum_{v\in V} tw_{vt}$ (h) is the value of total waiting time for all ETs, indicating the charging service level. The negative sign and the weight coefficient λ before $\sum_{t\in T}\sum_{v\in V} tw_{vt}$ are used to adjust the relationship between the ET service and charging service. In this research, we set λ to the average travel speed of all roads across a whole day in the city reported by the Shenzhen transportation administration, which is 26 (km/h), with the goal to transform waiting time into travel distances for the second objective. Constraint (7) indicates that each taxi demand can be covered once only by a single ET. Constraint (8) requires that the total number of charging ETs at a given station and time cannot exceed the number of stakes at that station. This constraint introduces the temporal competition between ET charging actions. Constraint (9) specifies that the charging service at a station is available only when that charging station is chosen to be located. Constraint (10) requires that the number of charging stations to be located is equal to M. Constraint (11) indicates that the travel distance of v between consecutive charging events is proportional to the cost electricity $\left(e_{t'}^v - e_t^v\right)$ over the time period $[t,t']$ in accordance with the assumption in equation (1). Because $e_{t'}^v$ and e_t^v are in the range [0, E], the limitation of the ET range is also specified. Constraints (12), (13), (14), and (15) impose integrality conditions on decision variables.

4.4 The genetic optimization procedure

Location problems are difficult to solve due to their inherent complexity. The heuristic algorithm is a promising method for complex location problems. Genetic algorithms evolve to globally optimal solutions for complex optimization problems by simulating natural behavior (Mitchell and Melanie, 1996). Therefore, this method has been successfully applied to many location problems (Xiao, 2008; Tong and Murray, 2009). In the present study, we employ a genetic algorithm to solve the STDCLM.

Genetic algorithms involve several components, namely, genome coding, population generation, fitness function, and selection, crossover, mutation, and stopping criteria. For the STDCLM, we use an integer representation to encode sited locations as a chromosome. The code length of a genome is equal to the number of located stations. The bit value indicates which the candidate places has been selected for a charging station. The objective function of the STDCLM (equation (6)) serves as the fitness function of each individual. An initial population of selected locations is randomly generated. At each generation, the roulette wheel selection is conducted according to the fitness value. Crossover is accomplished by the single point crossover operator. Mutation is employed at some random bits. Simulated evolution is repeated until the maximum number of iterations N_{max}^{1} have been reached or the objective (equation (6)) has not been improved over a fixed number of iterations N_{max}^{2}. Finally, the optimal results are reported, and the corresponding charging stations are displayed. Details concerning the demand coverage, ET charging, and essential waiting at the located stations are also obtained.

Before optimizing the STDCLM, the parameters of genetic algorithm, such as the population size p, the selection rate α, the mutation rate β, N_{max}^{1}, and N_{max}^{2}, are established after intensive experiments using the parameter tuning method of Coy et al. (2001). The top-k locations with the greatest taxi demands are generated as candidate places.

4.5 Analysis of results

According to the performance of used ET BYD E6 in Shenzhen, China, we set the maximum travel distance D_{max} to 250 km, the charging speed CS to E/120 min^{-1}. An initial scenario (S0) with 12 charging stations and 2,000 ETs was designed to assess the proposed approach. The obtained result is analyzed from both spatial and temporal perspective, including the spatial distribution of covered taxi demands, and the temporal patterns of ET serving, charging and waiting behaviors. The impact of charging speed is investigated by solving the scenario S0 with different settings of the parameter CS, from E/240 min^{-1} to E/60 min^{-1}. To evaluate the marginal utility of various numbers of sited charging stations, another four scenarios (S1-S4) were also designed and solved. Scenarios S1 and S2 are with 4 and 8 stations, respectively, whereas S3 and S4 are with 16 and 20 stations, respectively. The setting of each scenario, including the name, the number of ETs, the number of located stations, the number of stakes, and the ratio between ETs and stakes, is presented in Table 2.

To evaluate the environmental effect of the ET service, the daily RCE is also estimated using the evaluation model of Barth and Boriboonsomsin (2008), which estimates the carbon emission per mile of a light-duty internal combustion vehicle according to the running speed. As the ET releases zero carbon emission to air, we measured the ET's RCE with the carbon emission generated by an oil-taxi travelling the same route. So, with the speed information and the travel path obtained from the taxi GPS data, the amount of RCE owing to ET covered taxi demands is calculated. By accumulating all the RCE on road segments, we map the green effect of the ET system based on the number of ETs and the located charging stations.

[place Tab. 2 about here]

5. Experiment and results

5.1 Spatial-temporal distribution of taxi demands

Fig. 4 displays the temporal variation and the spatial distribution of taxi demands, and the aggregation of taxi travel flow for Shenzhen based on taxi GPS data. Fig. 4a indicates that the quantity of taxi demands per hour changes from 4,260 in the hour range [5:00, 6:00] to 25,660 in the hour range [22:00, 23:00]. Three taxi demand peaks are observed in the morning interval of [9:00, 11:00), in the evening interval of [14:00, 16:00), and in the night interval of [22:00, 23:00). Fig. 4b demonstrates that taxi demands are also non-uniform spatially. Most taxi demands are aggregated in the south and west Shenzhen, such as the downtown area, the airport, the railway station, and ports to Hong Kong. Demand is low in the north area, and nearly no demand appears in east Shenzhen, which is a nature reserve area. Fig. 4c illustrates the taxi travel flow. Such temporal and spatial dynamics lead to uneven taxi service requests in the city. Fig.5 shows the candidate nodes that have the highest taxi demand for charging station siting.

[place Fig. 4 about here]

[place Fig. 5 about here]

5.2 The obtained result

The obtained results from the scenario S0 are summarized in Table 3, where it is demonstrated that the 2,000 ETs served 69,151 taxi demands, or about 15.6% of 443,201 total daily taxi demands, and traveled a total of 928,240.7 km each day. The total distance traveled while specifically covering demands was 642,300.3 km, or about 69.2% (i.e., 642,300.3/928,240.7) of the total daily traveling distance by ETs. The ET's limited range is evident by a total of 5,530 charging actions requiring 9,382.4 total hours in a day. On average, each ET charged 2.765 (i.e., 5,530/2,000) times per day for an average charging time of 1.70 h (i.e., 9,382.4/5,530), which is clearly a key issue in the siting of ET charging stations. Because numerous ETs travel to charging stations simultaneously, 2,033 waiting actions for a total of 1,193.9 h of waiting occurred at the 12 stations employed in the scenario, or about 36.8% (i.e., 2,033/5,530) of all daily charging actions. The average waiting time was 0.59 hours (i.e., 1,193.9/2,033).

Fig. 6 displays the optimized locations of the 12 charging stations. Five stations (s1–s5) are located in the downtown area with the highest density of taxi demands. Three stations (s6–s8) are located in the west high-technology innovation area with a higher density of demands. Three stations (s9–s11) are located in Buji, a sub-center area of the city of Shenzhen. Only a single station (s12) is located in Longhua to provide essential ET service for taxi demands in north Shenzhen.

[place Tab. 3 about here]

[place Fig. 6 about here]

5.3 The spatial pattern and temporal pattern analysis of the obtained result

The spatial distribution of the covered taxi demands by ETs is displayed in Fig. 7. The results indicate that a relatively small number of stations can support the ET service for the entire city. Most of these demands are spatially aggregated in the downtown area. Some places, like the airport, the railway stations, and ports to Hong Kong also have intensive covered demands. However, much dispersed covered demands are observed in other areas like the north and east Shenzhen. Fig. 8 displays the spatial distribution of the ET covered ratio obtained by dividing the count of ET covered taxi demands to the total demands in the same place in the city, based on Fig. 4b. In contrast to the spatial aggregation observed for the covered taxi demands, the ratio distribution is quite spatially homogeneous. The ratios over most areas of the city are in the range [10%, 20%]. A ratio of less than 10% is observed in a small area in northeast Shenzhen. Ratios greater than 20% are observed for only a few areas at the border of the covered area, where taxi demands are quite few, as shown in Fig. 4b. Therefore, in these places, when two or three demands are covered by ETs, as shown in Fig. 7, the ratios will be high as shown in Fig. 8.

[place Fig. 7 about here]

[place Fig. 8 about here]

In addition to the spatial dynamics, the ET service on the road and the charging service at the stations also exhibit highly temporal dynamics. Fig. 9a illustrates the temporal variation of ET service on the roads. Following the taxi demand rhythm, the ET coverage peaks are in the periods [8:00, 10:00] and [15:00, 22:00]. However, the lower period of demand coverage occurs during [11:00, 13:00] because of the large number of ETs that travel to charging stations for first charging during that period, which leads to a decreased ET service on the road. Fig. 9b displays the varying ET charging behaviors at the located charging stations. In contrast to the rhythm of demand servicing shown in Fig. 9a, two charging peaks are observed in the periods [11:00, 14:00] and [21:00, 1:00], a few hours later than the peaks in demand serving on the roads. Such a temporal dynamic feature validates the necessity for including the time dimension in the proposed STDCLM.

The temporal dynamic of ET waiting is shown to be similar to that of charging, as indicated by Fig. 9c, where two waiting peaks are observed in the daily ET lifecycle. The first peak occurs in the period [12:00, 14:00], one hour later than the first charging peak, whereas the other peak occurs in the period [22:00, 3:00], just after the nighttime charging peak. Therefore, taxi demand coverage on the road, ET charging, and waiting at charging stations can be significantly influenced by temporal variations of the taxi demand in the city, none of which can be considered or analyzed in point demand or flow demand location approaches.

[place Fig. 9 about here]

5.4 Impact of charging speed

Table 4 presents the obtained results of scenario S0 with different charging speeds. It indicates that the faster the charging speed *CS* is, the better the obtained results are. As the charging speed improves from $E/240\ \text{min}^{-1}$ to $E/60\ \text{min}^{-1}$, the total charging actions of 2000 used ETs at 4 located stations increase from 4,390 to 6,146, while the total charging time per day decreases from 11,758.3 h to 4,172.5 h and the total waiting time sharply decreases from 4507.7 h to 17.8 h. As the ET spends will spend more time on the roads, the improvement of charging service at stations generates a better ET service on the roads. Total travel distance of covered demands increases from 476, 469.7 km to 662, 930.8 km.

[place Tab. 4 about here]

5.5 Marginal utility of located ET charging stations

Fig. 10 and Table 5 depict the objectives of each scenario and their tendencies as a function of the located stations. With the charging service supply increasing from S1 to S4, the obtained solutions exhibit a uniform improvement in both the ET service on the roads and the charging service at stations. For the ET service, the total length of ET covered travel increases from 403,707.3 km (S1) to 659,167.1 km (S4). For the charging service, the total waiting time reduces from 8,930.3 h with 1,939 waiting actions (S1) to 121.1 h with 498 actions (S4). Meanwhile, the total charging time increases from 4,448.4 h (S1) to 9,836.6 h (S4). The total number of charging actions increases from 2,733 (S1) to 5,777 (S4). The average charging time at the stations also increases from 1.63 h to 1.70 h, which is due to the reduced distance to a station with a greater number of charging stations.

It is noteworthy that new stations may induce an increase in the number of waiting actions. As shown in Table 5, the number of waiting actions at stations is nearly doubled between scenarios S1 (1,939 waiting actions) and S2 (3,619 waiting actions). This is mainly due to the inadequate charging service supply under the conditions in S1, in which each ET charges 1.367 times (i.e., 2,733/2,000) on average with 4 charging stations. With the addition of 4 more stations in S2, the charging service supply increases, and each ET charges an average of 2.52 times (i.e., 5,040/2,000) per day, which also generates an increased number of waiting actions at the stations. Nevertheless, the total waiting time still decreases from 8,930 h (S1) to 4,379 h (S2), as illustrated in Fig. 10. The average waiting time is also significantly improved from 4.61 (i.e., 8,930.3/1,939) h to 1.21 (i.e., 4,379/3,619) h between scenarios S1 and S2. This truth validates the improvement of the objectives with more charging stations.

However, the marginal utility of more located charging stations diminishes. Between scenarios S1 (4 stations) and S2 (8 stations), both the ET service on the road and the charging service at the stations significantly improve with more stations. The increase of the total distance of ET covered travel between S1 and S2 is 147,481.6 (i.e., 551,188.8−403,707.2) km. The increase of total charging time at located stations is 3,984.8 (i.e., 8,469.2−44,484.4) h. The decrease of the total waiting time is 4,551.3 (i.e., 8,930.3−4,379) h. However, with respect to the differences between scenarios S3 (16 stations) and S4 (20 stations), the improvement of the total distance of ET covered travel is only 14,937.6 (i.e., 657,263.0−642,325.4) km. The increase of total charging time is only 263 (i.e., 9,615.4−9,352.4) h. The decrease of total waiting time is 1,078.4 (i.e., 1,199.5−121.1) h.

Fig. 11 illustrates the positions of the located charging stations for the 5 scenarios considered. The distributions of located stations are observed to be very different with respect to the different numbers of sited stations. Charging stations initially appear along main roads in S1 (Fig. 11a). With increasing number of charging stations, new stations tend to be located in the high density taxi demand areas in S2 (Fig. 11b) and S0 (Fig. 11c). Finally, new stations are sited at the airport or low density taxi demand areas in northern Shenzhen in S3 (Fig. 11d) and S4 (Fig. 11e).

[place Tab. 5 about here]

[place Fig. 10 about here]

[place Fig. 11 about here]

5.6 Mapping the reduced carbon emission

Table 6 summarizes the total daily RCE when operating 2,000 ETs in conjunction with the varying number of charging stations associated with scenarios S0–S4. The table indicates that ET use can reduce daily carbon emission from about

211,118.1 to 339,891.4 kg depending upon the number of charging stations employed. Fig. 12 illustrates the spatial distribution of the daily RCE. In accordance with the ET footprint, reduced RCE is observed over nearly the entire road network. The most prominent effects occur in the downtown area (A), corridors to the downtown area (B), and the highway to the airport (C). Once again, the green effect obtained with more located charging stations diminishes. Between scenarios S1 (4 stations) and S2 (8 stations), the total RCE increases by 104,999.7 kg, and a more uniformly distributed green effect is generated. However, the total RCE only increases by 1,275.1 kg between scenarios S3 (16 stations) and S4 (20 stations) because the charging supply provided by 16 stations in S3 is nearly sufficient for the 2000 ETs used. Differences between the spatial RCE distributions in Fig. 12d and Fig. 12e are also very slight.

[place Tab. 6 about here]

[place Fig. 12 about here]

6. Conclusion

The electrification of public transportation has been a pioneer in attaining the goal of green transportation. With respect to the electric taxi (ET), one key to success lies in the location of charging stations to provide a high quality ET service for the public and a convenient charging service for ET drivers (Jung et al., 2014). However, in the dynamics of taxi demand and ET charging, time becomes a crucial factor, which is neglected in current location approaches that consider only spatial issues.

In recognition of this limitation, this article has addressed the location problem of ET charging stations by presenting a novel spatial-temporal demand coverage location approach. Detailed taxi demand data that captures spatial-temporal taxi request dynamics have been extracted from massive spatial-temporal GPS data for Shenzhen, China. The ET demand coverage is identified according to the spatial-temporal path that models the cyclic interaction between taxi demands, ETs, and charging stations. The objective of the presented spatial-temporal demand coverage location model (STDCLM) is to maximize the ET service on the roads and the charging service at the stations. This approach enables the siting of charging facilities in a spatial-temporal context rather than merely a spatial context. Experiments in Shenzhen, China not only demonstrate the effectiveness of the proposed location approach, but also validate the essential nature of the temporal dimension in taxi demand representation and the presented STDCLM. It has been shown that the optimized siting of charging stations can improve both the ET service on the roads and the charging service at stations. The estimation of daily RCEs also illustrates the environmental effect of ETs in conjunction with the located ET charging stations.

The main contributions of this research are three fold, as follows. Firstly, a novel location model was presented from the spatial-temporal perspective, which extends current location approach to address dynamic demand rather than static demand. Additionally, the complex interaction between travel demand and transportation service supply has been handled in a spatial-temporal context. Secondly, this research makes use of massive GPS data to support public policy making in transportation sectors, which acknowledges the value of big data and advances towards smart decisions in a highly dynamic environment. Thirdly, the problem of optimizing siting of ET charging stations has been addressed. This work can not only support short-term decision making regarding the use of ETs as a public utility, but can also help to promote the long-term development of the electric vehicle (EV) market.

Clearly, the results offered by the proposed approach are of great practical use for ET charging station siting. Nevertheless, the approach also demonstrates some notable limitations. Firstly, the located stations are only aimed at servicing ETs, and private EVs are not considered. In the future, the presented work should be extended towards the fulfillment of the charging requests of all EVs. The second limitation is the neglect of the variability of taxi demand. If taxi service is absent for a time, taxi demand nearby bus stations or metro stations may transfer to the bus or the metro system. Therefore, more public transportation data must be collected and be further involved in the presented work. The third limitation is the disregard for the relation between charging stations and grids. More data regarding grid infrastructure should be collected, and the candidate ET charging station sites should be adjusted accordingly. The last limitation is about the parameter λ, which is set to the mean travel speed of all roads across a whole day. However, urban traffic varies significantly across space and time (Li et al., 2011), leading to quite different reduced travel distances of the waiting. Hence, a spatial-temporal dependent value should be set according to historical traffic information in the further.

Acknowledgements

This research was supported in part by the National Science Foundation of China (Grants No. #41401444, #41231171, #41371377, #41271400), Shenzhen Dedicated Funding of Strategic Industry Development Program (#JCYJ20121019111128765), Shenzhen Basic Research Program (JCYJ20140828163633980), China Postdoctoral Science Foundation (2014M560671). The authors also would like to thank the anonymous reviewers and Professor Michael Kuby for their valuable comments and suggestions.

Reference

Barth, M., Boriboonsomsin, K., 2008. Real-World Carbon Dioxide Impacts of Traffic Congestion. Transportation Research Record: Journal of the Transportation Research Board 2058(1), 163-171.

Biazaran, M., SeyediNezhad, B., 2009. Center Problem. In: Zanjirani Farahani, R., Hekmatfar, M. (Eds.), Facility Location, Physica-Verlag, pp. 193-217.

Capar, I., Kuby, M., Leon, V. J., Tsai, Y.-J., 2013. An arc cover–path-cover formulation and strategic analysis of alternative-fuel station locations. European Journal of Operational Research 227 (1), 142-151.

Carpenter, T., Curtis, A., Keshav, S., 2014. The return on investment for taxi companies transitioning to electric vehicles. Transportation 41 (4), 785-818.

Church, R. L., 2002. Geographical information systems and location science. Computers & Operations Research 29 (6), 541-562.

Church, R., ReVelle, C., 1974. The maximal covering location problem. Papers in

Regional Science 32(1), 101-118.

Church, R.L., Murray, A.T., 2009. Business site selection, location analysis, and GIS. John Wiley & Sons.

Coy, S., Golden, B., Runger, G., Wasil, E., 2001. Using Experimental Design to Find Effective Parameter Settings for Heuristics. Journal of Heuristics 7(1), 77-97.

Cruz-Zambrano, M., Corchero, C., Igualada-Gonzalez, L., Bernardo, V., 2013. Optimal location of fast charging stations in Barcelona: A flow-capturing approach. In Proceeding of 2013 10th International Conference on the European Energy Market (EEM), pp. 1-6.

Drezner, Z., Hamacher, H. W., 2004. Facility location: applications and theory. Springer Verlag.

EPA office of transportation and air quality. http://www.epa.gov/otaq/

Fang, Z., Shaw, S.L., Tu W., LI, Q.Q., 2015. Spatiotemporal critical Opportunity and Link Identification for Joint Participation Scheduling. In: Kwan, M.-P., Richardson, D., Wang, D., Zhou, C (Eds). Space-Time Integration in Geography and GIScience. Springer, pp. 109-126.

Fang, Z., Shaw, S.-L., Tu, W., Li, Q., Li, Y. 2012. Spatio temporal analysis of critical transportation links based on time geographic concepts: a case study of critical bridges in Wuhan, China. Journal of Transport Geography 23, 44-59.

Fang, Z., Tu, W., Li, Q., Li, Q., 2011. A multi-objective approach to scheduling joint participation with variable space and time preferences and opportunities. Journal of Transport Geography 19(4), 623-634.

Frade, I., Ribeiro, A., Goncalves, G., Antunes, A. P., 2011. Optimal Location of Charging Stations for Electric Vehicles in a Neighborhood in Lisbon, Portugal. Transportation Research Record 2252, 91-98.

García-Palomares, J.C., Gutiérrez, J., Latorre, M., 2012. Optimizing the location of stations in bike-sharing programs: A GIS approach. Applied Geography 35(1), 235-246.

Gentili, M., Mirchandani, P.B., 2012. Locating sensors on traffic networks: Models, challenges and research opportunities. Transportation Research Part C: Emerging

Technologies 24, 227-255.

Goodchild, Michael F., Noronha, Valerian T., 1987. Location-allocation and impulsive shopping: the case of gasoline retailing. In: Ghosh, A., Rushton, G. (Eds.), Spatial Analysis and Location-Allocation Models. van Nostrand Reinhold, New York, pp. 121–136.

Hägerstrand, T., 1970. What about people in regional science? Papers in Regional Science 24(1), 6-21.

Hakimi, S. L., 1964. Optimum Locations of Switching Centers and the Absolute Centers and Medians of a Graph. Operations Research 12(3), 450-459.

Hiwatari, R., Ikeya, T., Okano, K., 2011. A road traffic simulator to analyze layout and effectiveness of rapid charging infrastructure for electric vehicle. In 2011 IEEE Vehicle Power and Propulsion Conference (VPPC), pp. 1-6.

Hodgson, M. J, 1990. A Flow-Capturing Location-Allocation Model. Geographical Analysis 22(3), 270-279.

IEA, 2013. Global Electric Vehicle Outlook. http://www.iea.org/publications/globalev outlook_ 2013.pdf. [Accessed at Oct 16, 2014]

IEA, 2014a. Tracking Clean Energy Progress 2014. http://www.iea.org/publications /freepublications/publication/Tracking_clean_energy_progress_2014.pdf. [Accessed at Oct 16, 2014]

IEA. 2014b. EV City Case book. http://www.iea.org/topics/transport/subtopics/electri cvehiclesinitiative/EVI_2014_Casebook.pdf. [Accessed at Oct 18, 2014]

Jung, J. Y., Chow, J. Y. J., Jayakrishnan, R., Park, J. Y., 2014. Stochastic dynamic itinerary interception refueling location problem with queue delay for electric taxi charging stations. Transportation Research Part C: Emerging Technologies 40, 123-142.

Kim, J. G., Kuby, M., 2013. A network transformation heuristic approach for the deviation flow refueling location model. Computers & Operations Research 40(4), 1122-1131.

Kuby, M., 2006. Prospects for geographical research on alternative-fuel vehicles. Journal of Transport Geography 14(3), 234-236.

Kuby, M., Lines, L., Schultz, R., Xie, Z., Kim, J.-G., Lim, S., 2009. Optimization of hydrogen stations in Florida using the Flow-Refueling Location Model. International Journal of Hydrogen Energy 34(15), 6045-6064.

Li, Q., Zhang, T., Yu, Y., 2011. Using cloud computing to process intensive floating car data for urban traffic surveillance. International Journal of Geographical Information Science 25(8), 1303-1322.

Li, X., He, J., Liu, X., 2009. Ant intelligence for solving optimal path-covering problems with multi-objectives. International Journal of Geographical Information Science 23(7), 839-857.

Lim, S., Kuby, M., 2010. Heuristic algorithms for siting alternative-fuel stations using the Flow-Refueling Location Model. European Journal of Operational Research, 204(1), 51-61.

Liu, L., Andris, C., Ratti, C., 2010. Uncovering cabdrivers' behavior patterns from their digital traces. Computers, Environment and Urban Systems 34(6), 541-548.

Miller, H. J., 1996. GIS and geometric representation in facility location problems. International Journal of Geographical Information Systems 10(7), 791-816.

Mitchell, Melanie, 1996. An Introduction to Genetic Algorithms. Cambridge, MA: MIT Press.

Murray, A.T., 2010. Advances in location modeling: GIS linkages and contributions. Journal of Geographical Systems 12(3), 335-354.

Nie, Y., Ghamami, M., 2013. A corridor-centric approach to planning electric vehicle charging infrastructure. Transportation Research Part B: Methodological 57, 172-190.

NYC TLC. 2013. Electric Vehicle Pilot Program. http://www.nyc.gov/html/tlc/html /news/initiative_ev_pilot_program.shtml#HowDoElectricVehiclesCharge. [Accessed at Aug 7, 2015]

Qian, X., Ukkusuri, S. V., 2015. Spatial variation of the urban taxi ridership using GPS data. Applied Geography 59, 31-42.

Qin, H., Zhang, W., 2011. Charging scheduling with minimal waiting in a network of electric vehicles and charging stations. In Proceedings of the Eighth ACM international workshop on Vehicular inter-networking. ACM, Las Vegas, Nevada, USA, pp. 51-60.

Rahmani, M., Jenelius, E., Koutsopoulos, H.N., 2015. Non-parametric estimation of route travel time distributions from low-frequency floating car data. Transportation Research Part C: Emerging Technologies. DoI: 10.1016/j.trc. 2015.01.015.

ReVelle, C. S., Eiselt, H. A., 2005. Location analysis: A synthesis and survey. European Journal of Operational Research 165 (1), 1-19.

Sathaye, N., 2014. The optimal design and cost implications of electric vehicle taxi systems. Transportation Research Part B: Methodological 67, 264-283.

Shenzhen Transportation Administration. 2012. Shenzhen Urban Transportation White Paper. http://www.sztb.gov.cn/xxgk/ghjh/fzgh /201205/t20120530_702. htm. [Accessed at Aug 7, 2015]

The BYD Auto Co.Ltd official website. http://www.bydauto.com.cn/car-param -e6.html. [Accessed at Oct 7, 2014]

IPCC. The fifth assessment report of IPCC. 2013. http://report.mitigation2014.org/sp m/ipcc_wg3_ar5_summary-for-policymakers_approved.pdf [Accessed at Oct 16, 2014]

Thill, J.C., 2000. Geographic information systems for transportation in perspective. Transportation Research Part C: Emerging Technologies 8(1), 3-12.

Tong, D., Murray, A. T., 2009. Maximizing coverage of spatial demand for service. Papers in Regional Science 88, 85-97.

TU, W., Fang, Z., Li, Q., 2010. Exploring time varying shortest path of urban OD pairs based on floating car data. In 2010 18th International Conference on Geoinformatics, Geoinformatics 2010, IEEE Computer Society, Beijing, China.

Upchurch, C., Kuby, M., 2010. Comparing the p-median and flow-refueling models for locating alternative-fuel stations. Journal of Transport Geography 18(6), 750-758.

Wang, Y.-W., Wang, C.-R., 2010. Locating passenger vehicle refueling stations. Transportation Research Part E: Logistics and Transportation Review 46(5),

791-801.
Wei, R., Murray, A. T., 2014. Evaluating Polygon Overlay to Support Spatial Optimization Coverage Modeling. Geographical Analysis 46(3), 209-229.
Wong, R. C. P., Szeto, W. Y., Wong, S. C. 2014. A cell-based logit-opportunity taxi customer-search model. Transportation Research Part C: Emerging Technologies 48, 84-96.
Xi, X., Sioshansi, R., Marano, V., 2013. Simulation–optimization model for location of a public electric vehicle charging infrastructure. Transportation Research Part D: Transport and Environment 22, 60-69.
Xiao, N., 2008. A unified conceptual framework for geographical optimization using evolutionary algorithms. Annals of the Association of American Geographers 98(4), 795-817.
You, P.-S., & Hsieh, Y.-C., 2014. A hybrid heuristic approach to the problem of the location of vehicle charging stations. Computers & Industrial Engineering, 70, 195-204.
YUE, Y., Lan, T., Yeh, A.G.O., LI, Q.Q., 2014. Zooming into individuals to understand the collective: A review of trajectory-based travel behavior studies. Travel Behavior and Society 1(2), 719-723.
Zeng, W., Castillo, I., Hodgson, M. J., 2010. Aggregating Data for the Flow−Intercepting Location Model: A Geographic Information System, Optimization, and Heuristic Framework. Geographical Analysis 42 (3), 301-322.
Zhan, X., Hasan, S., Ukkusuri, S.V., Kamga, C., 2013. Urban link travel time estimation using large-scale taxi data with partial information. Transportation Research Part C: Emerging Technologies 33, 37-49.
Zhang, J.D., Xu, J., Liao, S.S., 2013. Aggregating and Sampling Methods for Processing GPS Data Streams for Traffic State Estimation. IEEE Transactions on Intelligent Transportation Systems 14(4), 1629-1641.
Zhou Z., Lin T., 2012. Spatial and Temporal Model for Electric Vehicle rapid charging demand. In proceeding of Vehicle Power and Propulsion Conference (VPPC), 2012 IEEE, pp. 345-348.

Figure

Figure List:

Fig.1. Study area in the city of Shenzhen, China

Fig.2. The workflow of the spatial-temporal demand coverage approach

Fig.3. The interaction of taxi demands, electric taxis (ETs) and charging station in the spatial-temporal context.

Fig.4. The varying of spatial-temporal characteristic of taxi demands in Shenzhen, China. (a) The temporal variation of taxi demand. (b) The spatial distribution of taxi demand (counts/km^2). (c) The taxi travel flow in Shenzhen. All sub-figures are generated using the results from massive taxi GPS data.

Fig.5. Candidate places for siting charging stations.

Fig.6. The optimized location of the 12 charging stations

Fig.7. The spatial distribution of electric taxi (ET) covered taxi demands. The obtained count of covered demands are summarized in 1km × 1km cells.

Fig.8. The ratio of electric taxi (ET) covered taxi demands to the total of all taxi demands.

Fig.9. Electric taxi (ET) service on the road, charging, and waiting at the stations. The data are summarized from the obtained results. (a) The ET serving. (b) Charging at stations (h). (c) Waiting at stations (h).

Fig.10. The objectives of the STDCLM for scenarios with different number of charging stations.

Fig.11. The optimized locations of charging stations for scenarios given in Table 2

Fig.12. The spatial distribution of daily reduced carbon emission (RCE) of the electric taxi (ET) system (kg/km^2)

Fig.1. Study area in the city of Shenzhen, China

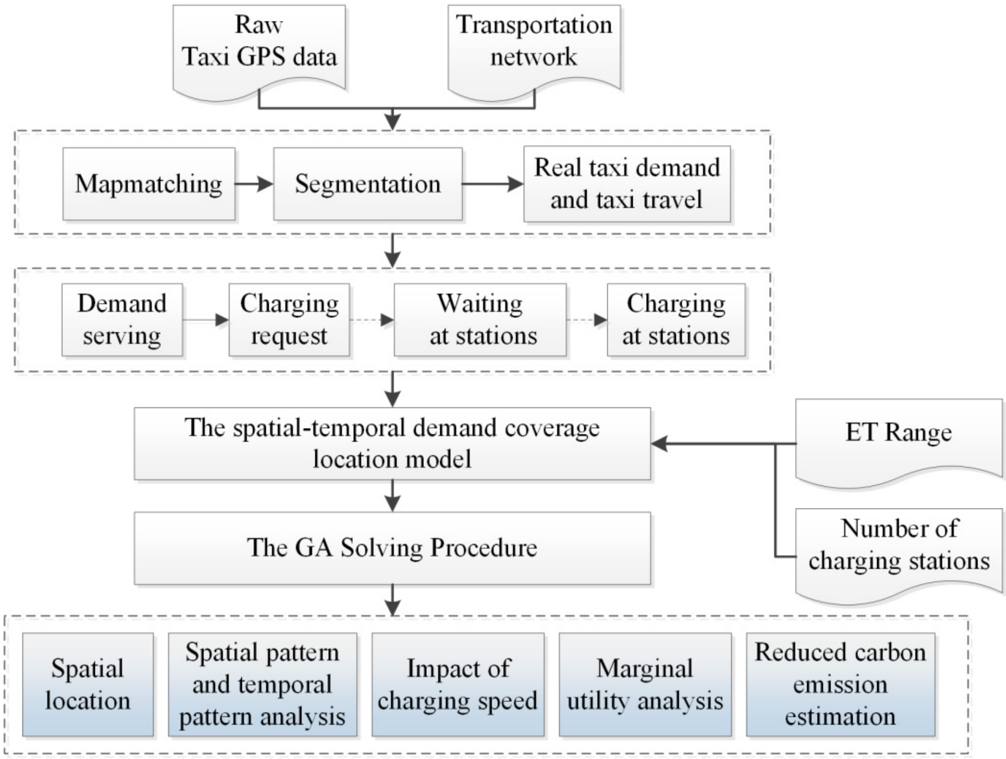

Fig.2. The workflow of the spatial-temporal demand coverage approach

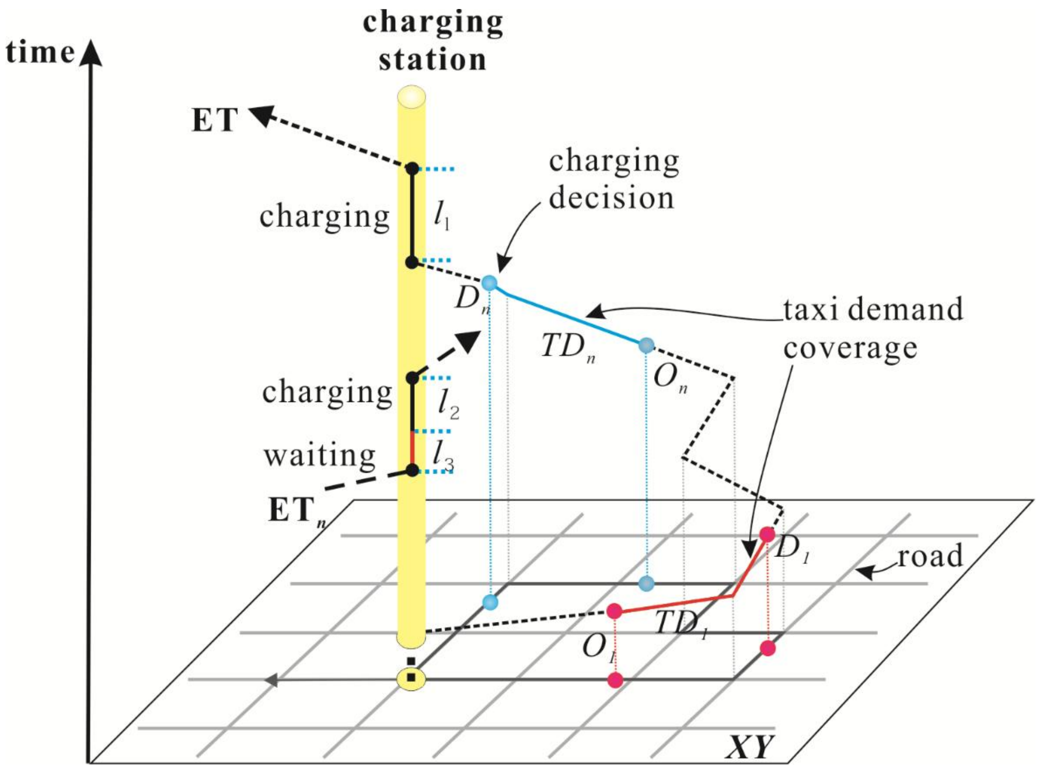

Fig.3. The interaction of taxi demands, electric taxis (ETs) and charging station in the spatial-temporal context.

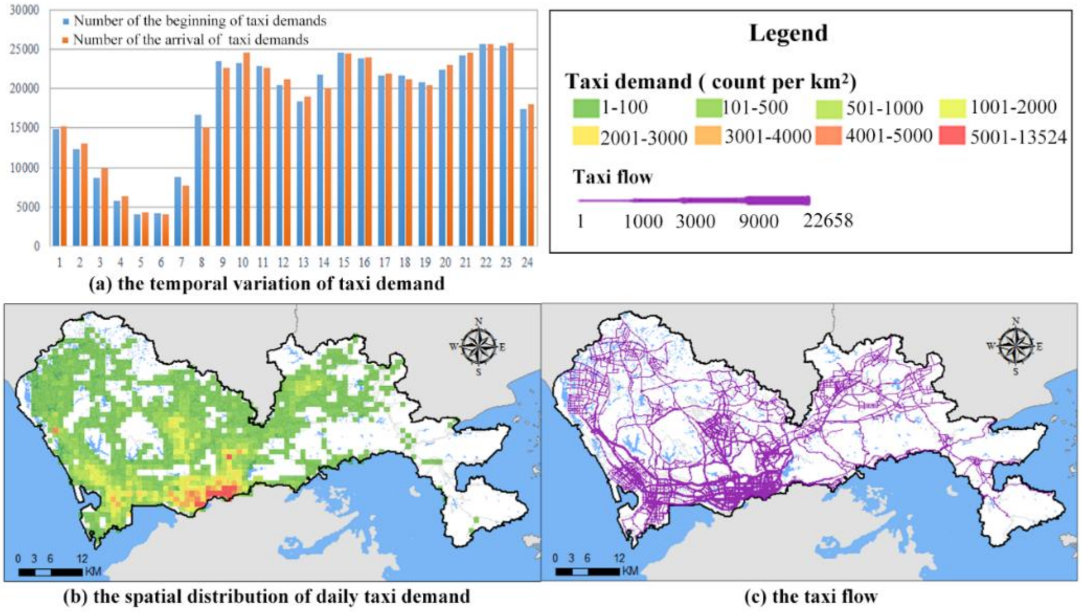

Fig.4. The varying of spatial-temporal characteristic of taxi demands in Shenzhen, China. (a) The temporal variation of taxi demand. (b) The spatial distribution of taxi demand (counts/km^2). (c) The taxi travel flow in Shenzhen. All sub-figures are generated using the results from massive taxi GPS data.

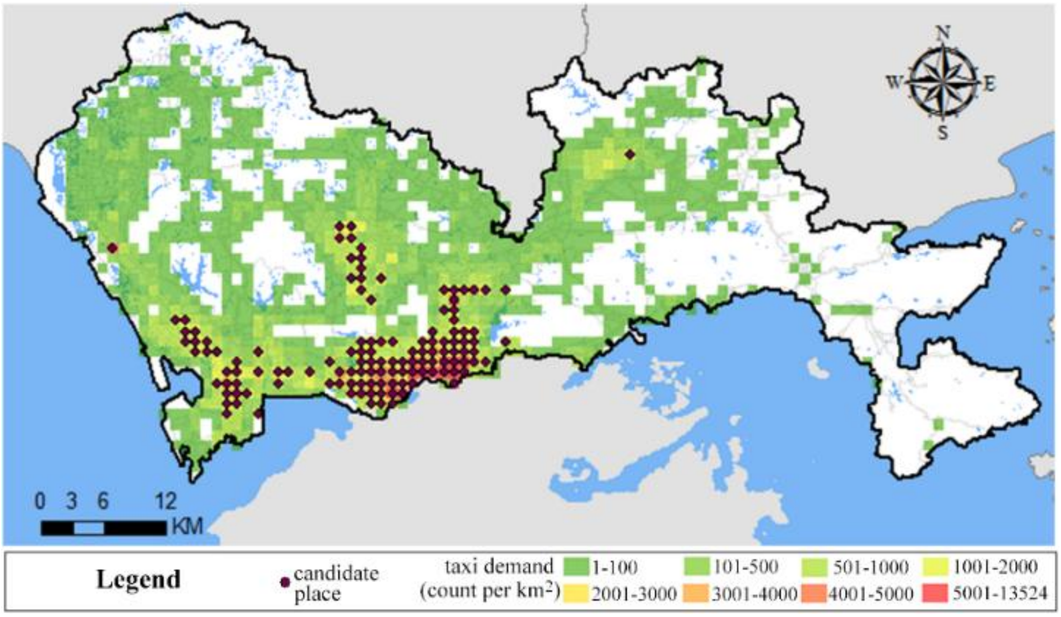

Fig.5. Candidate places for siting charging stations.

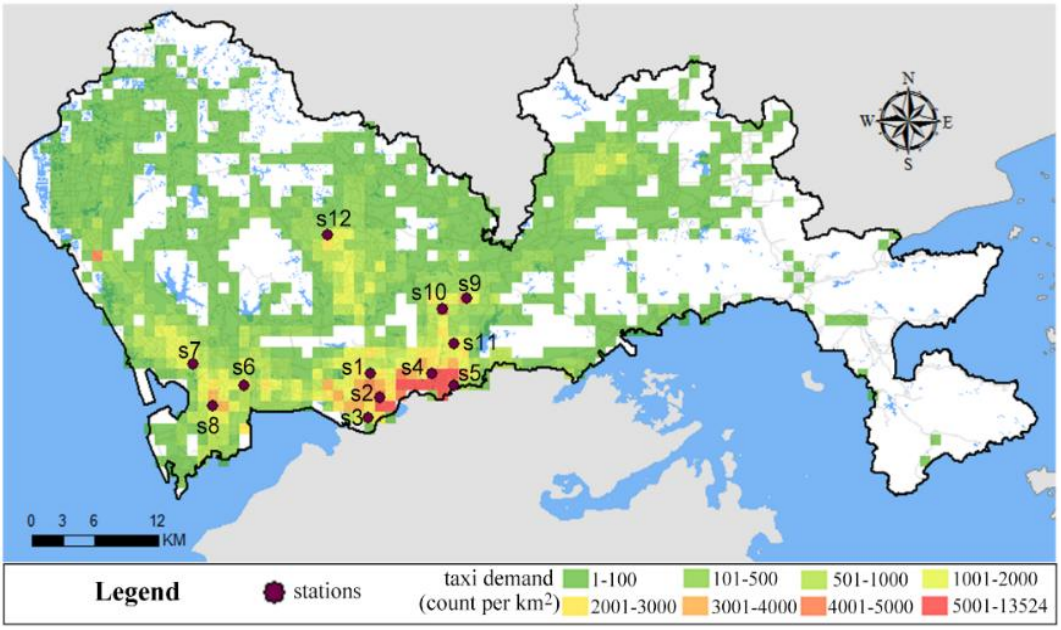

Fig.6. The optimized location of the 12 charging stations

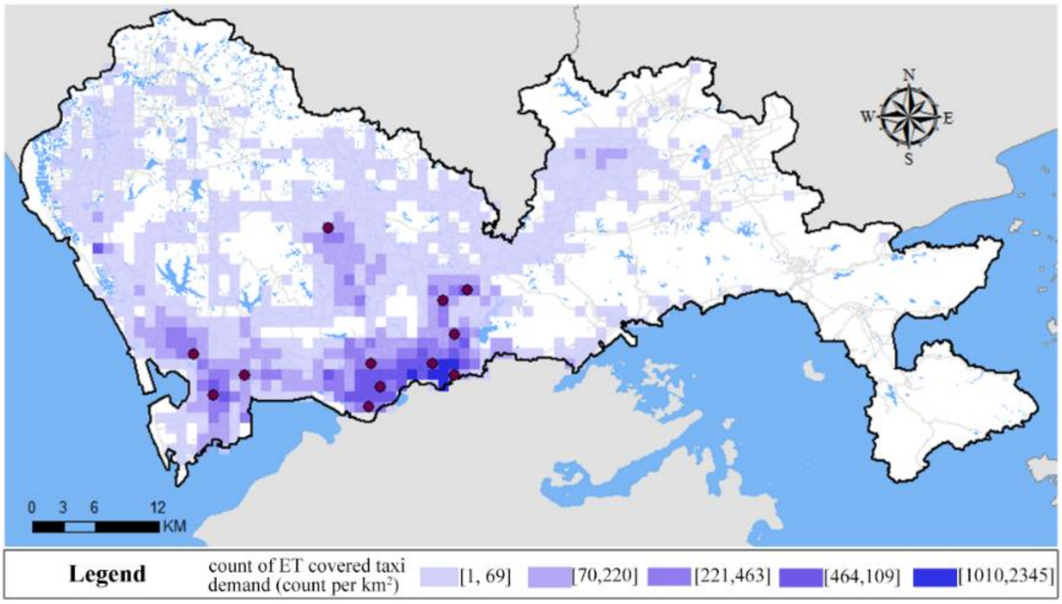

Fig.7. The spatial distribution of electric taxi (ET) covered taxi demands. The obtained count of covered demands are summarized in 1km × 1km cells.

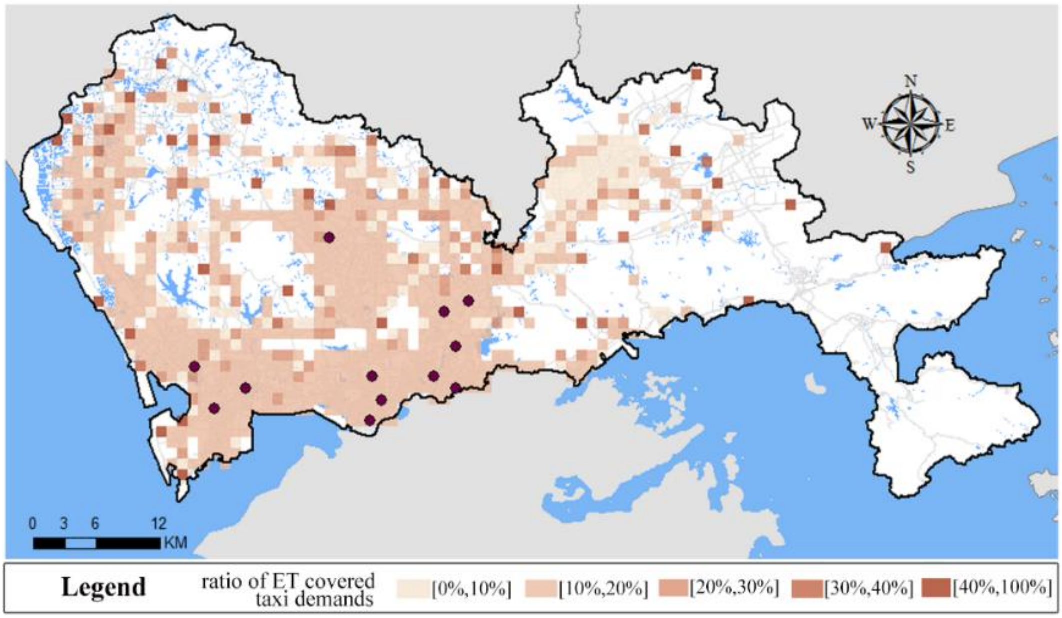

Fig.8. The ratio of electric taxi (ET) covered taxi demands to the total of all taxi demands.

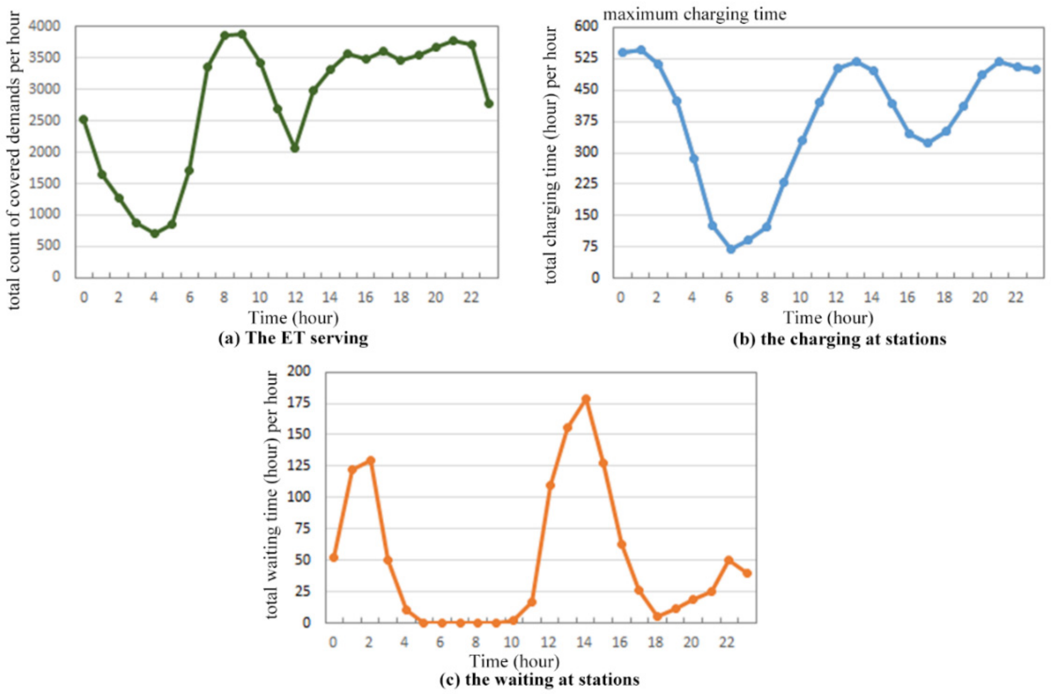

Fig.9. Electric taxi (ET) service on the road, charging, and waiting at the stations. The data are summarized from the obtained results. (a) The ET serving. (b) Charging at stations (h). (c) Waiting at stations (h).

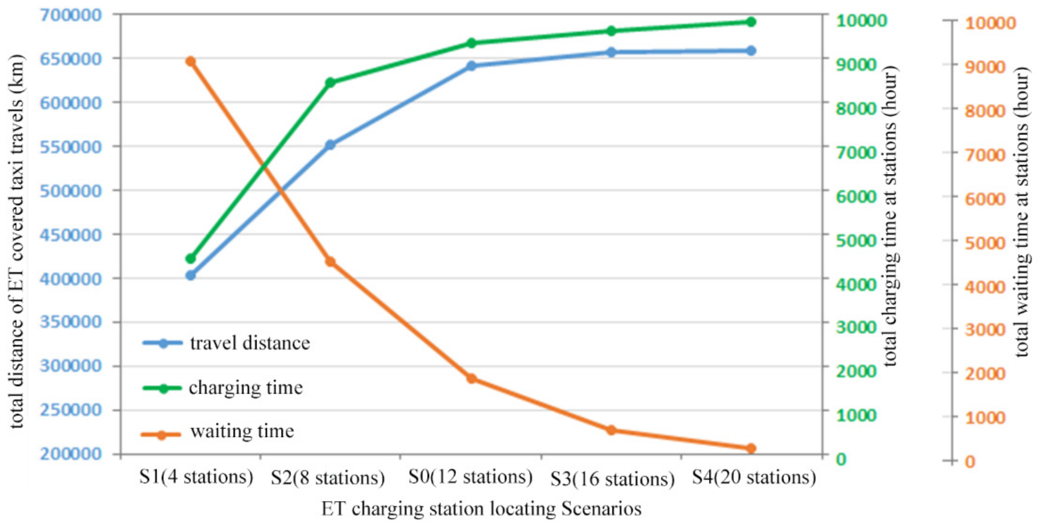

Fig.10. The objectives of the STDCLM for scenarios with different number of charging stations.

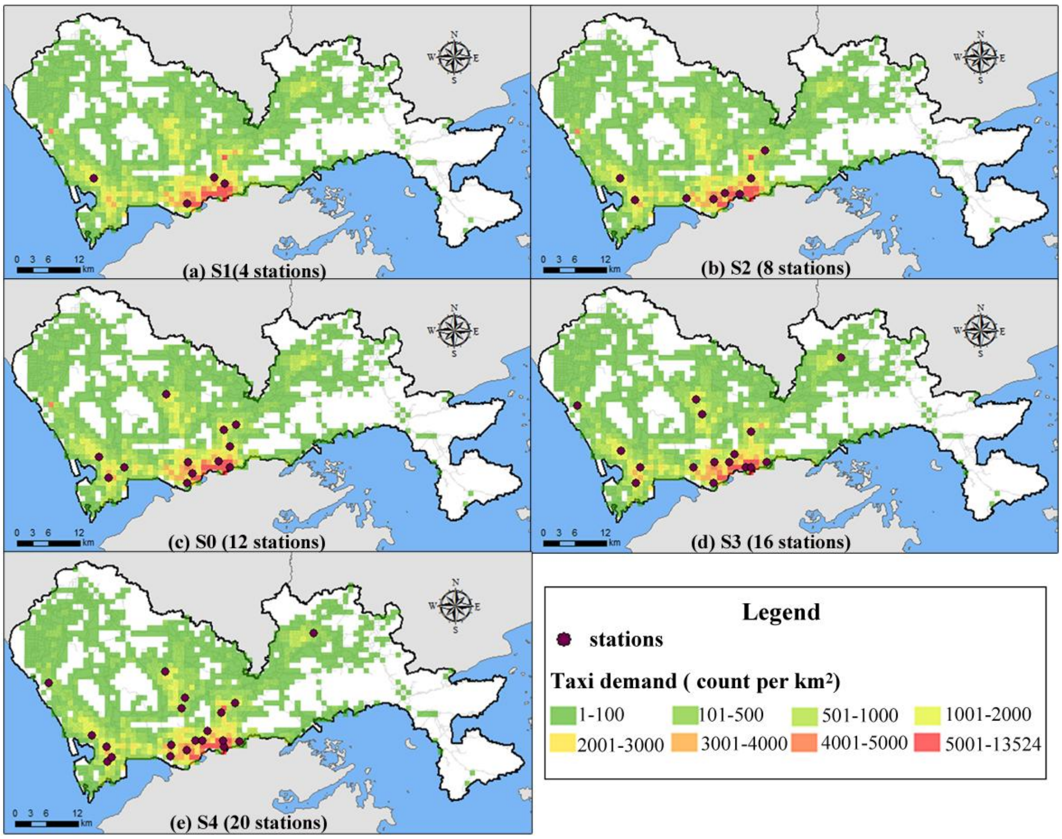

Fig.11. The optimized locations of charging stations for scenarios given in Table 2

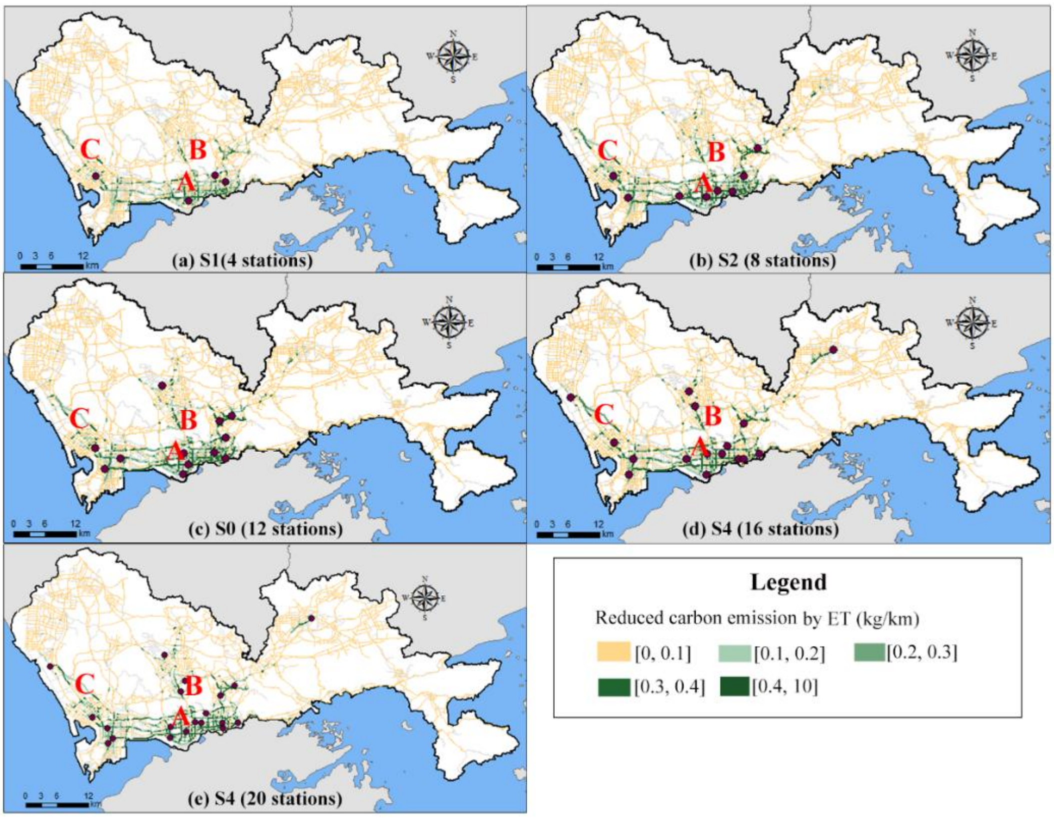

Fig.12. The spatial distribution of daily reduced carbon emission (RCE) of the electric taxi (ET) system (kg/km^2)

Table list

Table 1

The format of taxi GPS data in the city of Shenzhen, China.

ID	VID	Time stamp(/sec)	Longitude	Latitude	Status	Speed (m/s)
106411231324	11011	200	113.928***	22.505***	0	12.0
106411231325	8648	280	113.930***	22.515***	0	6.2
…	…		…	…	…	…
106411231998	11011	2000	113.419***	22.539***	1	12.0
106411253724	11011	2040	113.419***	22.540***	0	4.8
106411263340	14899	2041	113.411***	22.603***	0	9.2

Table 2

The setting of the electric taxi (ET) charging stations siting scenarios

Scenarios	Number of ETs	Number of stations	Number of stakes	Ratio(ETs: stakes)
S0	2000	12	600	10:3
S1	2000	4	200	10:1
S2	2000	8	400	10:2
S3	2000	16	800	10:4
S4	2000	20	1000	10:5

Table 3

The setting and the result of the ET charging stations location scenario

Scenario Setting		**Results**	
Scenario	S0	Total travel distance of all ETs per day (km)	928240.7
Number of ETs	2000	Total travel distance of covered demands per day (km)	642300.3
Number of Stations	12	Total number of ET covered demand per day	69151
Number of charging stakes in a station	50	Total charging time at stations per day (hour)	9382.4
Total number of charging stakes	600	Total number of charging actions per day	5530
Ratio (ETs: stakes)	10:3	Total waiting time at stations per day (hour)	1193.9
		Total number of waiting actions per day	2033

Table 4

The variation of objectives with charging speeds

Charging speed *CS* (*E*/min^{-1})	***E*/240**	***E*/180**	***E*/120**	***E*/60**
Total travel distance of covered demands (km)	476469.7	542849.3	642300.3	662930.8
Total charging time at stations (hours)	11758.3	10379.1	9382.4	4172.5
Total number of charging actions per day	4390	5137	5530	6146
Total waiting time at stations (hours)	4507.7	2682.0	1193.9	17.8
Total number of waiting actions per day	2229	2466	2033	97

Table 5

Daily charging and waiting of ETs at charging stations

Scenario	Num of ETs	Num of stations	Num of charging actions	Average charging time (/hour)	Num of waiting actions	Average waiting time (/hour)
S1	2000	4	2733	1.63	1939	4.61
S2	2000	8	5040	1.68	3619	1.21
S0	2000	12	5530	1.69	2033	0.59
S3	2000	16	5665	1.70	1068	0.51
S4	2000	20	5777	1.70	498	0.24

Table 6

The reduced carbon emission (RCE) by ETs for scenarios given in Table 2

Scenario	Num of ETs	Num of stations	Total RCE (/kg)	Change in RCE (/kg)
S1	2000	4	211118.1	-
S2	2000	8	316117.8	104999.7
S0	2000	12	330174.2	14056.4
S3	2000	16	338616.3	8442.1
S4	2000	20	339891.4	1275.1